head with wider bandwidth. MPT-induced 'breathing' of one channel at the expense of the other allowed us to estimate a PDL of ~1.8dB, mostly due to the EDFAs. In an optimal average-power limited system with small PDL, the associated worst-case penalty equals ~1/2 of the PDL value in decibels. The BER was measured in the RX at 2.5Gbit/s by demultiplexing a regenerated 10Gbit/s signal. Transmission was nearly error-free (1 error in 45mm at 2.5Gbit/s, i.e. BER 1.5×10^{-13}).
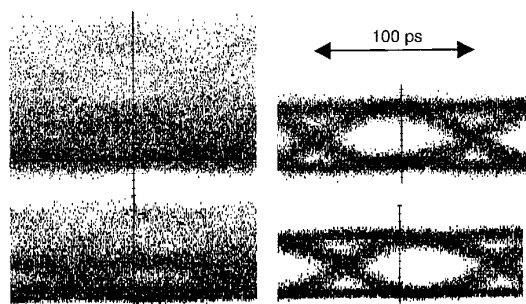

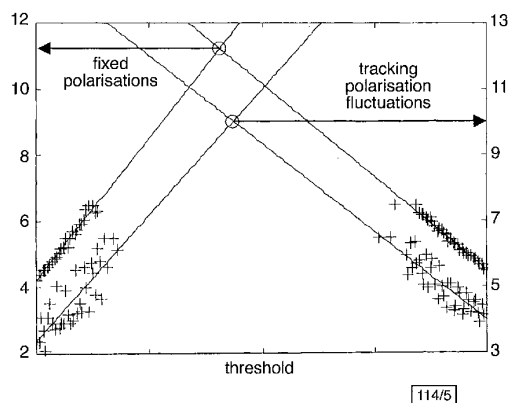Fig. 4 *Eye diagrams corresponding to Fig. 2 (left) and Fig. 3 (right)*

Fig. 5 *Q factors back-to-back (top), and with rotating MPT (bottom; vertically offset)*

A decision-circuit threshold was scanned. Extrapolation of the measured Q values ≥ 3 yielded Q factors of 11.2 back-to-back and 10 with slowly rotating MPT, respectively (Fig. 5).

Each polarisation transformer was accessed in intervals of 1.2ms. A ten-fold speed increase could be obtained without shortening the measurement intervals if data transfer times to an external PC (presently 80% of the time) were eliminated, and if one microcontroller were provided per channel.

PolDM detection is also possible if each receiver branch maximises the autocorrelation product $\langle b_1 i_1 \rangle$, $\langle b_2 i_2 \rangle$ between its decision circuit input and output signals (dotted lines in Fig. 1). This was also tried, with results virtually identical to Figs. 3 and 4 right.

Conclusions: 2×10 Gbit/s PolDM transmission has been demonstrated with equal optical and clock frequencies in the two channels, for the first time to our knowledge. The signals are acquired using correlation products. PDL (1.8dB) and endless polarisation changes (~1rad/s speed) in the transmission fibre are supported.

S. Hinz, D. Sandel, R. Noé and F. Wüst (*Optical Communications and High-Frequency Engineering, Electrical Engineering and Information Technology, University of Paderborn, Warburger Str. 100, 33098 Paderborn, Germany*)

E-mail: noe@uni-paderborn.de

References

1 HILL, P.M., OLSHANSKY, R., and BURNS, W.K.: 'Optical polarization division multiplexing at 4Gb/s', *IEEE Photonics Technol. Lett.,* 1992, **4**, pp. 500–502

2 HEISMANN, F., HANSEN, P.B., KOROTKY, S.K., RAYBON, G., VESELKA, J.J., and WHALEN, M.S.: 'Automatic polarization demultiplexer for polarisation-multiplexed transmission systems'. ECOC 1993, Montreux, Switzerland, 1993, Paper WeP9.3, pp. 401–404

3 NOÉ, R., SANDEL, D., and WÜST, F.: 'Polarization mode dispersion tolerance of bandwidth-efficient multilevel modulation schemes'. Optical Fiber Communications Conf. 2000, Baltimore, Maryland, USA, 5–10 March 2000, Paper WL4

4 CIMINI, L.J., HABBAB, I.M.I., JOHN, R.K., and SALEH, A.A.M.: 'Preservation of polarisation orthogonality through linear optical system', *Electron. Lett.,* 1987, **23**, (25), pp. 1365–1366

Optical switching by coherent collision of spatial solitons

J.A. Andrade-Lucio, B. Alvarado-Méndez, R. Rojas-Laguna, O.G. Ibarra-Manzano, M. Torres-Cisneros, R. Jaime-Rivas and E.A. Kuzin

The authors study experimentally the coherent collision of two one-dimensional spatial bright solitons in a photorefractive crystal. Depending on the relative phase of the solitons and their intersecting angle, effects such as fusion, energy exchange and soliton birth have been observed. The experimental and numerical results are in good agreement.

Introduction: Spatial optical solitons have been suggested for all-optical guiding and switching in nonlinear-optical media. The predictions and observations of optical spatial solitons in nonlinear materials, which require considerably less laser power than Kerr-type materials, are the subject of increasing interest. Spatial solitons in photorefractive crystals (PRCs), for example, have been observed [1 – 4]. These soliton-induced waveguides can be used to guide and steer another optical beam, which in this case constitutes the simplest optical element. One of their more promising characteristics for practical applications in photonics are the structures formed by intersecting waveguides such as X or Y junctions [5, 6]. Such intersecting waveguides can be implemented by colliding two or more solitons. Recently collision between mutually incoherent 2D spatial solitons in an SBN crystal was reported in [7], interaction forces between one-dimensional spatial solitons in parallel propagation were observed in [8], and the fusion and birth of 2D spatial solitons caused by the collision and annihilation of photorefractive solitons was reported in [9, 10].
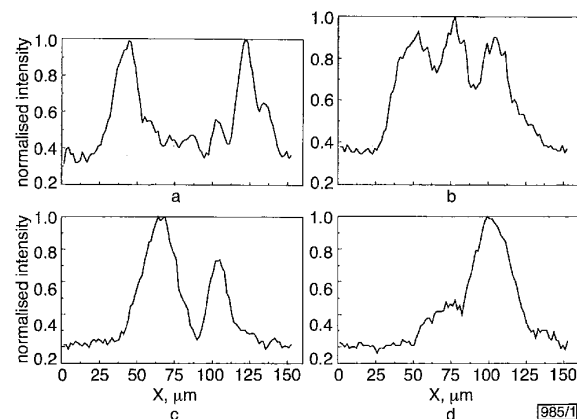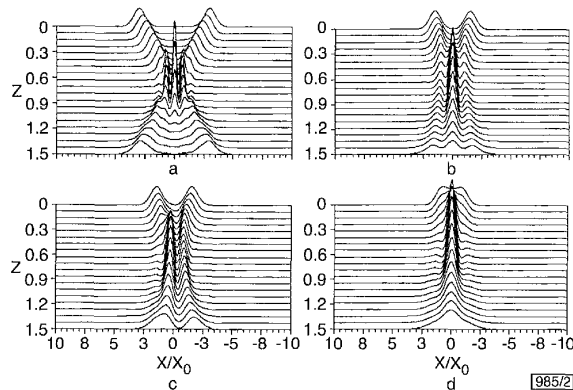

Fig. 1 *Experimental results between colliding solitons*

a 0.8° angle of collision and relative phase of 0rad
b 0.4° angle of collision and relative phase of 0rad
c 0.4° angle of collision and relative phase of $\pi/2$rad
d 0.2° angle of collision and relative phase of 0rad

Experimental results: The experimental setup used to study the soliton collision was similar to that used in our previous investigations of soliton interactions [8]. One He-Ne CW laser beam 1 (λ = 632.8nm) was expanded and collimated and split into two beams of equal intensity by means of a cube beam splitter and subsequently recombined. The two beams were focussed by means of a cylindrical lens. Separation of the beams was controlled using one of the mirrors of a Michelson interferometer. The relative phase between the beams was controlled by means of a mirror mounted upon a piezoelectric transducer, allowing for variable delay (and relative phase) between the two beams when a DC field drove the transducer. We obtained appropriate widths (13μm FWHM) for the beams arriving at the SBN crystal ($6 \times 6 \times 6$mm^3) by using the cylindrical lens. The trajectories of both beams were slightly convergent so that they would intersect symmetrically inside the crystal. The other He-Ne laser beam was expanded and collimated to illuminate the crystal uniformly. The intensity of this uniform beam was equal to the peak intensity of the focussed beams, i.e. μ $\simeq$ 1. The focussed beams were polarised parallel to the applied external field. The exit face of the crystal was viewed using a CCD camera and processed by a frame grabber in a personal computer.

Initially each beam was propagated separately in the biased crystal. A DC electric field (necessary for soliton formation under drift nonlinearity) was applied to the crystal parallel to its c axis. In most cases, an electric field of 2.3kV/cm was applied to the crystal when the input and the output widths of the beam were identical. This fact is a clear indication of the formation of a bright spatial soliton [1]. In the next step, we allowed both beams to intersect symmetrically inside the crystal. For different angles of collision, we found that for angles > 0.8°, the beams emerged from the collision virtually unchanged for different relative phase between them (see Fig. 1a). The strong phase sensitivity of the soliton collision was particularly evident after the intersection angle was decreased to < 0.8°. For example, for an angle of collision of 0.4°, effects such as the birth of a new beam and energy transfer were observed after collision for different relative phases among the solitons, as shown in Figs. 1b and c. For an angle of 0.2°, we observed fusion for 0rad of relative phase between the solitons, as shown in Fig. 1d.

Fig. 2 *Numerical results between colliding solitons*

a 0.8° angle of collision and relative phase of 0rad
b 0.4° angle of collision and relative phase of 0rad
c 0.4° angle of collision and relative phase of π/2rad
d 0.2° angle of collision and relative phase of 0rad

Numerical results: A scalar one-dimensional model of laser beam propagation through a PRC with drift nonlinearity yields the following equation for the beam envelope [11, 12]:

$$i\frac{\partial q}{\partial Z} = \frac{1}{2}\frac{\partial^2 q}{\partial X^2} + \mu R \frac{|q|^2}{1 + \mu|q|^2} q$$

where q represents the beam envelope normalised to $\sqrt{I_s}$, and I_s is the peak intensity of the initial beam. In this equation, $\mu = I_s/I_o$ is the saturation parameter, where I_o is the intensity of the uniform illumination provided to the crystal. $R = L_D/L_{NL}$, where $L_D = n_o k_o x_o^2$ is the diffraction length and $L_{NL} = 1/(k_o \delta n_o)$ is the characteristic nonlinear length. n_o is the linear refractive index, k_o is the wave number, x_o is the width of the initial beam envelope, and $\delta n_o = (1/2)rn_o^3 V_o/L$ is the nonlinear contribution to the refractive

index, where r is the electro-optic coefficient, V_o is the externally applied voltage, and L is the transverse width of the crystal. Finally, $X = x/x_o$ and $Z = z/L_D$.

We now compare the experimental results with those of the numerical solutions of this equation. We assume that the input beam follow the Gaussian profile, and $x_o = 13$μm. Using $n_o = 2.35$, we have $L_D = 3.94$mm and a normalised crystal length of $Z_{end} = 1.52$. For our SBN crystal, $r = 220$pm/V and $V_o = 1.4$kV. Therefore $R = 6$. For each angle of collision, we need to know the separation between the beams Δx, normalized to x_o, angle of collision or transversal velocity V, and the relative phase between them. The critical parameters for the numerical simulations are:

Angle of 0.8°: $\Delta x = 6$, $V = 3.94$, separation between beams of 78μm.

Angle of 0.4°: $\Delta x = 2.8$, $V = 1.82$, separation between beams of 36μm.

Angle of 0.2°: $\Delta x = 1.53$, $V = 1.01$, separation between beams of 20μm.

Fig. 2 shows the numerical results for 0.8° angle of collision and 0rad of relative phase between the solitons (Fig. 2a), 0.4° angle of collision and 0, π/2 of relative phase between the solitons (Figs. 2b and c), and finally 0.2° angle of collision and 0 rad of relative phase (Fig. 2d).

Conclusions: We have presented an experimental and numerical study of soliton collision in a photorefractive crystal. We have shown that this can result in energy transfer, birth of a new beam and repulsion, and have obtained good agreement between the experimental and numerical results. This result opens the way for designing optical switches or optical logic gates based on the collision of spatial solitons by properly choosing the relative phase between them.

J.A. Andrade-Lucio, E. Alvarado-Méndez, R. Rojas-Laguna, O.G. Ibarra-Manzano, M. Torres-Cisneros and R. Jaime-Rivas (*Facultad de Ingeniería Mecánica, Eléctrica y Electrónica, A.P.215-A, Salamanca Gto. 36730, Mexico*)

E-mail: andrade@salamanca.ugto.mx

E.A. Kuzin (*Instituto Nacional de Astrofísica, Óptica y Electrónica, A. P.51 y 216, C.P. 72000, Puebla, Pue, Mexico*)

References

1   DUREE, G.C., Jr., SHULTZ, J.L., SALAMO, G.J., SEGEV, M., YARIV, A., CROSIGNANI, B., DIPORTO, P., SHARP, J., and NEURGAONKAR, R.R.: 'Observation of self-trapping of an optical beam due to the photorefractive effect', *Phys. Rev. Lett.*, 1993, **71**, pp. 533–536
2   ITURBE-CASTILLO, M.D., MÁRQUEZ-AGUILAR, P.A., SÁNCHEZ-MONDRAGÓN, J.J., STEPANOV, S.I., and VYSLOUKH, V.: 'Spatial solitons in photorefractive Bi$_{12}$TiO$_{20}$ with drift mechanism of nonlinearity', *Appl. Phys. Lett.*, 1994, **64**, pp. 408–410
3   SEGEV, M., SALAMO, G., DUREE, G., MORIN, M., CROSIGNANI, B., DIPORTO, P., and YARIV, A.: 'Photorefractive dark and vortex solitons', *Opt. Photonics News*, 1994, **5**, p. 9
4   DUREE, G., MORIN, M., SALAMO, G., SEGEV, M., CROSIGNANI, B., DIPORTO, P., SHARP, B., and YARIV, A.: 'Dark photorefractive spatial solitons and photorefractive vortex solitons', *Phys. Rev. Lett.*, 1995, **74**, pp. 1978–1981
5   LUTHER-DAVIES, B., and YANG, X.: 'Waveguides and Y junctions formed in bulk media by using dark spatial solitons', *Opt. Lett.*, 1992, **17**, pp. 496–498
6   AKHMEDIEV, N.N., and ANKIEWICZ, A.: 'Spatial solitons X-junctions and couplers', *Opt. Comm.*, 1993, **100**, pp. 186–192
7   SHIH, M.F., and SEGEV, M.: 'Incoherent collision between two-dimensional bright steady-state photorefractive spatial screening solitons', *Opt. Lett.*, 1996, **21**, pp. 1538–1540
8   GARCÍA-QUIRINO, G.S., ITURBE-CASTILLO, M.D., VYSLOUKH, V.A., SÁNCHEZ-MONDRAGÓN, J.J., STEPANOV, S.I., LUGO-MARTINEZ, G., and TORRES-CISNEROS, G.E.: 'Observation of interaction forces between one-dimensional spatial solitons in photorefractive crystals', *Opt. Lett.*, 1997, **22**, pp. 154–156
9   KRÓLIKOWSKY, W., and HOLMSTROM, S.A.: 'Fusion and birth of spatial solitons upon collision', *Opt. Lett.*, 1997, **22**, pp. 369–371
10   KRÓLIKOWSKY, W., LUTHER-DAVIES, B., DENZ, C., and TSCHUDI, T.: 'Annihilation of photorefractive solitons', *Opt. Lett.*, 1998, **23**, pp. 97–99

11 SEGEV, M., VALLEY, G.C., CROSIGNANI, B., DIPORTO, P., and YARIV, A.: 'Steady state spatial screening-solitons in photorefractive materials with external applied field', *Phys. Rev. Lett.*, 1994, **73**, pp. 3211–3214

12 ITURBE-CASTILLO, M.D., SÁNCHEZ-MONDRAGÓN, J.J., VYSLOUKH, V.A., STEPANOV, S.I., CHÁVEZ-CERDA, S., and TORRES-CISNEROS, G.E.: 'Experimental evidence of modulation instability in a photorefractive Bi₁₂TiO₂₀ crystal', *Opt. Lett.*, 1995, **20**, pp. 1853–1855

Unrepeatered 160 Gbit/s RZ single-channel transmission over 160 km of standard fibre at 1.55 μm with hybrid MZI optical demultiplexer

R. Ludwig, U. Feiste, S. Diez, C. Schubert, C. Schmidt, H.J. Ehrke and H.G. Weber

The authors report on single-channel, single-polarisation, 160 Gbit/s, RZ, 1.55 μm transmission over 160 km of standard fibre without inline optical amplifiers, with passive compensation of dispersion and dispersion slope, and using an optical 160 to 10 Gbit/s demultiplexer based on a hybrid Mach-Zehnder interferometer.

Introduction: Installed fibre networks comprise predominantly non-dispersion-shifted fibre (standard fibre, SMF) exhibiting chromatic dispersion values $D = 16$ ps/km/nm at a wavelength of 1.55 μm in the window of an erbium-doped fibre amplifier (EDFA). There is an increasing interest in expanding existing WDM systems based on standard fibre transmission to high single-channel bit rates.

A prerequisite for high bit rate transmission over standard fibre is dispersion compensation. To date, the best dispersion compensation technique is based on dispersion-compensating fibre (DCF). There are many single-channel transmission experiments with data rates > 40 Gbit/s [1]. Using standard fibre, however, there are only few transmission experiments with data rates > 40 Gbit/s [2, 3].

In this Letter, we report on 160 Gbit/s RZ data transmission (single wavelength channel) over a transmission line, which comprises a single unrepeatered (no EDFA in the transmission line) standard fibre span with a length of 160 km (without DCF). This is the largest unrepeatered transmission span for a bit rate > 80 Gbit/s [3]. We used a DCF for dispersion compensation, which was fabricated and provided by Lucent Technologies Denmark A/S. This DCF enabled us to compensate for both chromatic dispersion D and the dispersion slope $S = dD/d\lambda$. The compensation of D and S is an essential ingredient for the transmission of single-channel bit rates of 40 Gbit/s and above [4] and for the simplification of WDM systems. Without changing the adjustment of the dispersion compensation, we show that the wavelength of the pulse source (the channel wavelength) can be tuned over at least 10 nm before the pulsewidth becomes too large for error-free 160 Gbit/s data transmission [3].
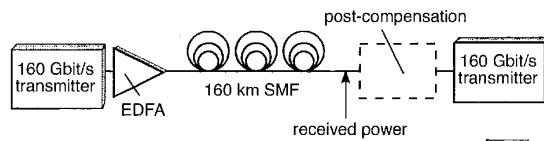

Fig. 1 Experimental setup

Experiment: The experimental setup is shown in Fig. 1. The 160 Gbit/s data transmitter comprised a tunable modelocked laser fabricated by LKF Advanced Optics GmbH, a modulator and a fibre delay line multiplexer. The modelocked laser generated a 10 GHz pulse train, which was intensity modulated with a pseudorandom bit sequence (PRBS $2^7 - 1$) using an external modulator. The 10 Gbit/s data signal was then multiplexed by a fibre delay-line multiplexer (four stages) to a 160 Gbit/s single polarisation data signal. To ensure a multiplexed PRBS data stream, the

bit sequences were shifted against each other by $(2^7 - 1)/n$ bit periods with $n = 2, 4, 8, 16$. The 160 Gbit/s data signal (wavelength 1.55 μm, pulsewidth 1.6 ps at the SMF input, transform-limited pulses) was transmitted over 160 km SMF (0.22 dB/km, PMD < 0.05 ps/√km). The DCF (27.3 km, 0.5 dB/km, $D_{DCF} = -98$ ps/nm/km, $S = -0.33$ ps/nm²/km, PMD < 0.18 ps/√km) was placed at the receiver (post-compensation) as in [3]. For the adjustment of the optimum dispersion compensation an additional section (7 km) of SMF was needed.
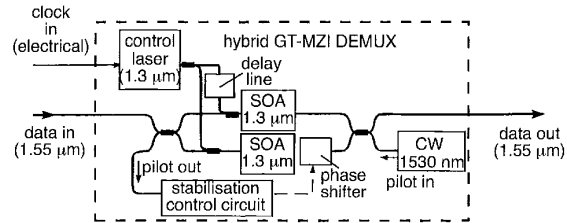

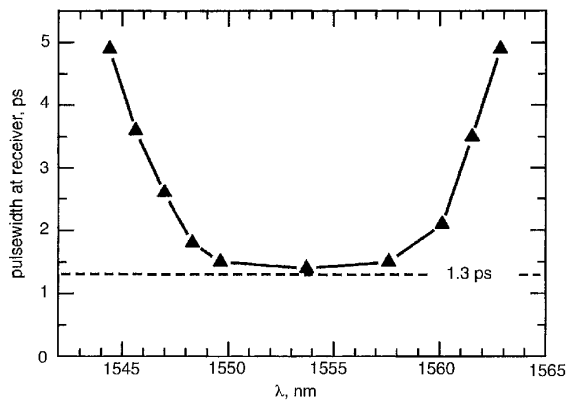*Fig. 2 Setup of Mach-Zehnder interferometer switch*

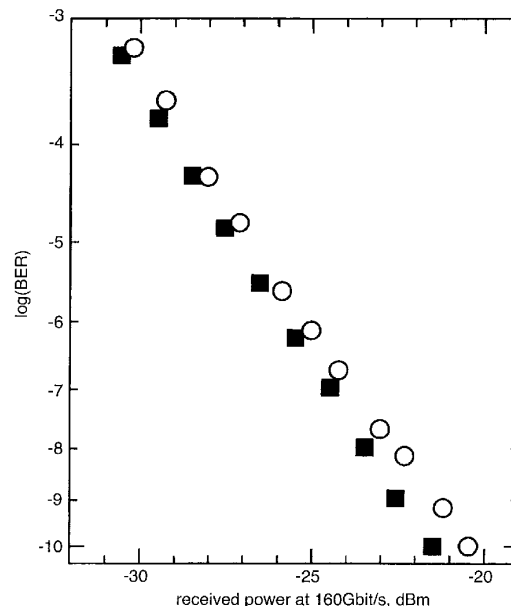*Fig. 3 Dependence of pulsewidth at receiver on wavelength*

Fig. 4 BER performance

■ back-to-back
○ 160 km SMF

In the receiver, the 160 Gbit/s data signal was optically demultiplexed to a 10 Gbit/s data signal using an optical switch based on a hybrid Mach-Zehnder interferometer (MZI) with semiconductor